Conserved small protein associates with the multidrug efflux pump AcrB and differentially affects antibiotic resistance

Errett C. Hobbs[a,1,2], Xuefeng Yin[a,b,1], Brian J. Paul[a,3], Jillian L. Astarita[a,4], and Gisela Storz[a,5]

[a]Cell Biology and Metabolism Program, Eunice Kennedy Shriver National Institute of Child Health and Human Development, Bethesda, MD 20892-5430; and [b]Health Science Center, Peking University, Beijing 100191, China

Edited by Hiroshi Nikaido, University of California, Berkeley, CA, and approved August 28, 2012 (received for review June 14, 2012)

The AcrAB–TolC multidrug efflux pump confers resistance to a wide variety of antibiotics and other compounds in *Escherichia coli*. Here we show that AcrZ (formerly named YbhT), a 49-amino-acid inner membrane protein, associates with the AcrAB-TolC complex. Copurification of AcrZ with AcrB, in the absence of both AcrA and TolC, two-hybrid assays and suppressor mutations indicate that this interaction occurs through the inner membrane protein AcrB. The highly conserved *acrZ* gene is coregulated with *acrAB* through induction by the MarA, Rob, and SoxS transcription regulators. In addition, mutants lacking AcrZ are sensitive to many, but not all, of the antibiotics transported by AcrAB–TolC. This differential antibiotic sensitivity suggests that AcrZ may enhance the ability of the AcrAB–TolC pump to export certain classes of substrates.

multidrug resistance | resistance-nodulation-division | RND superfamily

Antibiotic-resistant bacteria have been recognized as a threat to public health since the 1940s, when penicillin-resistant bacteria were first reported (reviewed in ref. 1). As the threat of antibiotic-resistant bacteria continues to expand, there is increased urgency to understand the mechanisms of resistance. Bacteria commonly rely on promiscuous efflux pumps, such as the AcrAB–TolC complex in *Escherichia coli* (reviewed in ref. 2), to export antimicrobial agents and on enzymes to inactivate specific compounds. Many bacteria also possess transcription factors, such as the homologous *E. coli* regulators MarA, Rob, and SoxS (3, 4), that respond to drugs by activating the expression of genes encoding proteins involved in antibiotic efflux and detoxification.

The *E. coli* AcrAB–TolC complex, which consists of the polytopic inner membrane protein AcrB, the periplasmic adaptor protein AcrA, and the outer membrane channel TolC, has been studied extensively as a model for multidrug efflux pumps (reviewed in ref. 5). The AcrB protein is a member of the resistance-nodulation-division (RND) superfamily found in all domains of life. AcrB forms a trimer with each of its monomers in a different state during the transport reaction (access, binding, and extrusion). Through a continuous transitioning between the three states, AcrB harnesses the proton motive force to pump compounds out of the cell from the inner membrane or periplasm through the TolC channel (6, 7).

In Gram-negative bacteria, polyspecific RND proteins transport all clinically used groups of antibiotics from the cell (reviewed in ref. 2) and, together with the outer membrane barrier, serve to make Gram-negative bacteria much more antibiotic resistant than their Gram-positive counterparts (5, 8). In addition to exporting the acridine dyes for which it is named, AcrB substrates include antibiotics such as chloramphenicol, β-lactams, tetracyclines, macrolides, fluroquinolones, rifampicin, fusidic acid, and novobiocin (5, 8, 9). AcrB can also export organic solvents such as cyclohexane, hexane, heptane, octane, and nonane, as well as detergents like SDS, bile salts, and Triton X-100.

Genes encoding small proteins (sproteins) of 50 amino acids or less in length are inadequately annotated in all organisms (reviewed in ref. 10). The *E. coli* chromosome contains ~60 confirmed sprotein-encoding genes (11). The physiological roles played by the majority of sproteins are unknown. However, many are highly conserved and/or are expressed under very specific environmental conditions (11, 12), implying that they perform important functions. More than half of the sproteins are predicted to contain an α-helical transmembrane (TM) domain (11), which suggests that one role for sproteins might be to modify the activities of larger membrane proteins.

In this study, we found that a functional epitope-tagged derivative of the previously uncharacterized 49-amino-acid YbhT protein, here renamed AcrZ, associates with the AcrAB–TolC efflux pump in an AcrB-dependent manner. Expression of *acrZ* is coregulated with *acrAB* and *tolC* by the MarA, Rob, and SoxS transcription factors. Consistent with the association and coregulation of AcrZ and AcrB, Δ*acrZ* cells are sensitive to a subset of antibiotics that affect Δ*acrB* mutants, albeit not to the same degree. We postulate that AcrZ may function by assisting the AcrAB–TolC pump in the recognition and export of a subgroup of substrates.

Results

AcrZ–SPA Copurifies with Components of the AcrAB–TolC Membrane Efflux Pump. The 49-amino-acid AcrZ is highly conserved among enterobacteria and other Gram-negative species (Fig. 1). The protein is predicted to contain an N-terminal TM helix (11, 13), and previous subcellular localization experiments have shown that tagged derivatives partition with the membrane fraction and that the C terminus is in the cytoplasm (13). Our group has used the sequential peptide affinity (SPA) tag (14) to observe the accumulation of multiple sprotein fusions (11). Because AcrZ–SPA is easily detected (11) and a strain producing the tagged derivative is phenotypically wild type in a cell envelope stress assay (15) as well as in the antibiotic sensitivity assays described below, AcrZ–SPA was a good candidate for biochemical approaches to identify interacting protein partners. Chromosomally expressed AcrZ–SPA was purified from a crude lysate of exponentially growing cells on the basis of the 3xFLAG tag and the calmodulin-binding peptide that compose the SPA tag. Two high-molecular-weight proteins consistently observed to copurify with AcrZ–SPA (Fig. 2) were identified as AcrB (114 kDa) and AcrA (42 kDa) by mass spectrometry. This finding indicated AcrZ associates with the AcrAB–TolC efflux pump, an interaction supported by the observation that AcrZ–SPA is detected in both the inner and the outer membrane fractions in a wild-type strain but is found

Author contributions: E.C.H., X.Y., B.J.P., J.L.A., and G.S. designed research; E.C.H., X.Y., B.J.P., and J.L.A. performed research; E.C.H., X.Y., B.J.P., J.L.A., and G.S. analyzed data; and E.C.H., X.Y., and G.S. wrote the paper.

The authors declare no conflict of interest.

This article is a PNAS Direct Submission.

[1]E.C.H. and X.Y. contributed equally to this work.

[2]Present address: Lawrence Livermore National Laboratory, Livermore, CA 94551.

[3]Present address: Biochemical Sciences & Engineering, DuPont Central Research and Development, Wilmington, DE 19880.

[4]Present address: Division of Medical Sciences, Harvard Medical School, Boston, MA 02115.

[5]To whom correspondence should be addressed. E-mail: storzg@mail.nih.gov.

This article contains supporting information online at www.pnas.org/lookup/suppl/doi:10.1073/pnas.1210093109/-/DCSupplemental.

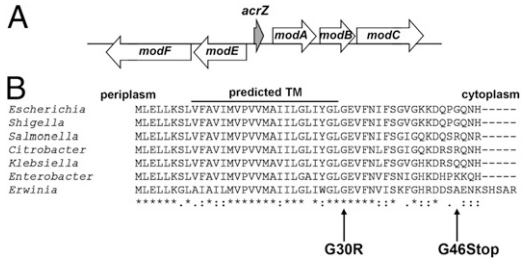

Fig. 1. AcrZ is a highly conserved transmembrane sprotein. (*A*) *acrZ* is located between two operons involved in molybdenum metabolism. (*B*) *acrZ* is present in virtually all enteric bacteria. The AcrZ protein contains one predicted TM domain at the N-terminal region (13). The sequences shown were aligned using ClustalW (http://www.ebi.ac.uk/Tools/msa/clustalw2/). Arrows indicate positions of two dominant-negative mutations. Based on an alignment with AcrB TM2 (Fig. S3*A*), the actual TM domain of AcrZ may correspond to amino acids 2–21 instead of 9–29 as predicted.

predominantly in the inner membrane fraction of an Δ*acrB* deletion strain (13).

AcrZ Associates with AcrAB–TolC via the Inner Membrane Protein AcrB. We verified the interaction of AcrZ–SPA with the AcrAB–TolC complex by performing a reciprocal purification of AcrZ-SPA with AcrB-His_6 (a functional C-terminal hexahistidine-tagged fusion protein of AcrB). As shown in Fig. 3*A*, AcrZ-SPA is coeluted from the Ni^{2+}-NTA column in the eluate fraction with AcrB–His_6 from the *acrZ-SPA acrB-His*$_6$ lysate, but not from the *acrZ-SPA* lysate. As a control, we carried out a similar purification with His_6-tagged PhoR, an unrelated multitransmembrane protein. This experiment is complicated by the fact that untagged AcrB was found to copurify with other hexahistidine-tagged proteins due to the histidine-rich cluster on its surface (16). Indeed, both AcrB and AcrZ-SPA were found to copurify with PhoR–His_6 from a *phoR-His*$_6$ strain carrying wild-type *acrAB* (Fig. S1*A*). However, AcrZ-SPA did not copurify with PhoR–His_6 from the corresponding strain lacking *acrAB* (Fig. S1*A*), providing further support that AcrZ–SPA interacts specifically with AcrB. The level of AcrZ–SPA was notably lower in the Δ*acrAB* mutant, suggesting that the binding with its target may be required for AcrZ stability.

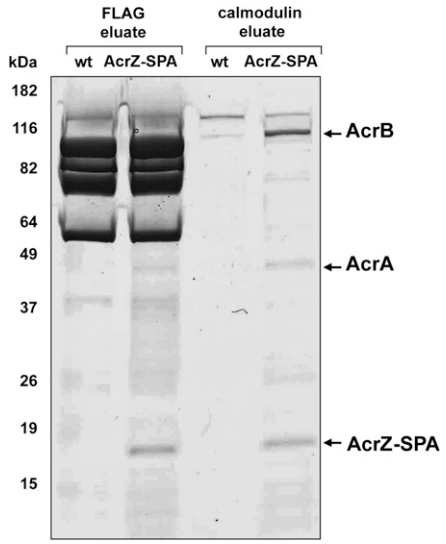

Fig. 2. AcrZ–SPA interacts with members of the AcrAB–TolC efflux pump. The interacting partners of a functional AcrZ-epitope fusion protein (AcrZ–SPA) were copurified by passing cell lysates over α-FLAG beads and calmodulin beads in a two-step process. Eluates from each column were subjected to SDS/PAGE. Bands enriched in lysates from cells containing AcrZ–SPA were excised from the gel and identified by mass spectrometry.

Importantly, AcrB–His_6 does not interact promiscuously with random small membrane proteins, as neither SPA-tagged YbgT nor SPA-tagged YccB was retained on Ni^{2+}-NTA resin in conjunction with AcrB–His_6 (Fig. S1*B*). We also found that AcrZ–SPA was retained by AcrB–His_6 on Ni^{2+}-NTA resin in the absence of both AcrA and TolC (Fig. 3*A*), indicating that AcrZ can associate with AcrB in the absence of the two other members of the AcrAB–TolC complex. Together, these results indicate that AcrZ–SPA is retained on the column by virtue of its association with AcrB.

To examine whether untagged AcrZ interacts with the AcrB pump, we also performed limited tryptic digestion of AcrB–His_6 purified from wild-type or Δ*acrZ* mutant cells. For AcrB–His_6 purified from wild-type cells, one fragment of ∼40 kDa was visible after 30 min of digestion (Fig. 3*C*). In contrast, for AcrB–His_6 purified from cells lacking AcrZ, the 40-kDa fragment appeared at 10 min of digestion, and one additional fragment of ∼100 kDa was detected after 30 min of digestion (Fig. 3*C*). This result suggests that the accessibility of AcrB is altered by untagged AcrZ, likely via a direct interaction.

Two Dominant-Negative Mutations Map to the C-Terminal Half of AcrZ. Dominant-negative mutants, which inhibit the function of the wild-type protein when the wild-type and mutant proteins are produced simultaneously, are useful in both biochemical and genetic approaches as they can be used to define the nature of a protein–protein interaction. We thus set out to identify dominant-negative mutations in *acrZ*. To this end, *acrZ* was amplified by error-prone PCR and cloned behind an arabinose-inducible promoter on pBAD24 (17). Wild-type cells transformed with mutagenized pBAD24-*acrZ* were first screened for growth under inducing conditions to ensure that the mutant versions of AcrZ were nontoxic to the cell.

As described below, Δ*acrZ* cells are sensitive to chloramphenicol. We exploited this phenotype in our screen for dominant-negative mutants by identifying cells that grew in the presence of chloramphenicol (at a concentration that is inhibitory to the growth of Δ*acrZ* cells) when expression of the plasmid-borne copy of *acrZ* was repressed (on plates containing glucose) but not when both the chromosomally encoded and plasmid-encoded copies of *acrZ* were expressed (on plates containing arabinose). Two robust dominant-negative mutations, which both mapped to the C-terminal half of AcrZ, were isolated. One missense mutation (G30R) altered a highly conserved glycine located at the C-terminal end of the α-helix to an arginine. The other mutation was a nonsense mutation that truncated the protein by four amino acids (G46Stop).

One possible explanation for the dominant-negative phenotype is that the mutations disrupt a productive interaction between wild-type AcrZ and AcrB. This could occur if the dominant-negative AcrZ mutants bind AcrB more tightly and occlude wild-type AcrZ. To test whether the SPA-tagged versions of either $AcrZ^{G30R}$ or $AcrZ^{G46Stop}$ are still capable of binding AcrB–His_6, we once again purified AcrB–His_6 on Ni^{2+}-NTA from lysates of cells that produce either the wild-type or the mutant forms of AcrZ–SPA. Similar to wild-type AcrZ–SPA, $AcrZ^{G46Stop}$–SPA interacts with AcrB–His_6 (Fig. 3*B*), suggesting that this dominant-negative mutant acts by sterically occluding wild-type AcrZ from AcrB and preventing a productive interaction. On the other hand, $AcrZ^{G30R}$–SPA did not copurify with AcrB–His_6 (Fig. 3*B*). This observation suggests that $AcrZ^{G30R}$ does not stably associate with AcrB. The mechanism by which this dominant-negative mutant blocks the activity of wild-type AcrZ is not known.

Suppressor Mutations Map to TM Helix 11 and the Cytoplasmic Domain of AcrB. To further examine the binding of AcrZ to AcrB as well as screen for *acrB* mutations that could suppress the $acrZ^{G30R}$ mutation, we tested for a direct interaction between AcrZ and AcrB using the bacterial two-hybrid system. Specifically, we assayed whether AcrZ and AcrB fused to the T18 and T25 fragments of *Bordetella pertussis* CyaA (18) could restore adenylate cyclase activity leading to increased β-galactosidase ac-

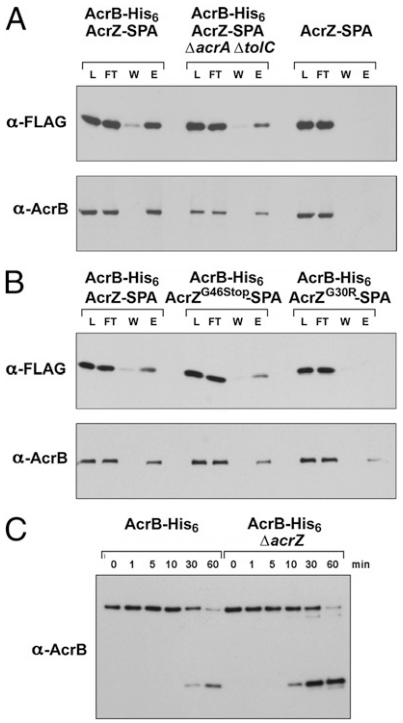

Fig. 3. AcrZ–SPA associates with AcrAB–TolC through an interaction with AcrB. (*A*) AcrZ–SPA only bound the Ni^{2+}-NTA resin when hexahistidine-tagged AcrB (AcrB–His_6) was present. (*B*) One dominant-negative form of AcrZ-SPA (G46Stop) associates with AcrB while the other dominant-negative form (G30R) does not. For *A* and *B*, cell lysates (L) were passed over Ni^{2+}-NTA resin, and the flow-through (FT) fractions were collected. Bound proteins were washed (W) with a 20-mM imidazole buffer and subsequently eluted (E) from the resin by using a 250-mM imidazole solution. All four fractions were subjected to SDS/PAGE and immunoblot analysis to detect SPA-tagged proteins (α-FLAG) or AcrB (α-AcrB). (*C*) AcrB–His_6 shows a differential trypsin digestion pattern in the presence of AcrZ. AcrB–His_6 was purified from wild-type *acrZ* or Δ*acrZ* cells and mixed with trypsin (500 mg/mL:1 mg/mL ratio) and incubated at 37 °C for 1, 5, 10, 30, or 60 min. Digestion products were separated on SDS/PAGE and subjected to immunoblot analysis with α-AcrB antibody.

tivity. Consistent with the results of the affinity purification assays, there was a strong interaction between wild-type AcrZ–T18 and T25–AcrB as evidenced by high levels of β-galactosidase activity compared with empty vector controls (Fig. 4*A*), whereas the G30R dominant-negative mutation in AcrZ–T18 abolished the interaction with T25–AcrB (Fig. 4*A*). The loss of β-galactosidase activity in the dominant-negative mutant cannot be attributed to a difference in protein amounts, as AcrZ–T18 and $AcrZ^{G30R}$–T18 accumulate to similar levels in the cell (Fig. S2).

To identify *acrB* mutations that could suppress the $acrZ^{G30R}$ mutation, we randomly mutated the *acrB*-coding sequence in the T25 construct and screened for mutants that restored an interaction with $AcrZ^{G30R}$–T18 in the two-hybrid assay. Two missense mutations in T25–AcrB were isolated and identified as H526Y and L984P. As shown in Fig. 4, β-galactosidase activity in strains coexpressing $AcrZ^{G30R}$–T18 with T25–$AcrB^{H526Y}$or $AcrZ^{G30R}$–T18 with T25–$AcrB^{L984P}$ was increased >10-fold compared with the $AcrZ^{G30R}$–T18 T25–AcrB strain to 23% (for H526Y) or 37% (for L984P) of wild-type levels. The H526Y suppressor mutation is in the cytoplasmic α-helix between TM6 and TM7, whereas the L984P suppressor mutation is in TM11 of AcrB (Fig. S3).

We also recombined the H526Y and L984P alleles into the chromosomal copy of *acrB* to test whether the mutant versions of AcrB could compensate for the chloramphenicol sensitivity introduced by pBAD24-encoded $AcrZ^{G30R}$. Consistent with the ability of the H526Y mutation to suppress the reduced binding of AcrB to $AcrZ^{G30R}$, we found that the suppressor mutation restored some resistance to chloramphenicol (Fig. 4*B*). Unfortunately, the strain expressing the L984P did not grow under the conditions of our assay and thus could not be tested.

***acrZ* Is Regulated by MarA, Rob, and SoxS.** *acrZ* shares strong synteny with *modEF* and *modABC*, two operons involved in molybdenum uptake and in regulating the synthesis of the molybdenum cofactor molybdopterin (Fig. 1*A*). In *E. coli*, molybdopterin is used (often in conjunction with Fe-S clusters) by ~20 molybdo-enzymes to conduct a broad range of redox reactions, including the detoxification of compounds such as aromatic aldehydes, in both the cytoplasm and the periplasm (reviewed in ref. 19).

In LB medium, AcrZ–SPA is most abundant in exponentially growing cells, but it is also present in cells harvested from both stationary phase and overnight cultures (11). Given its synteny with *modEF* and *modABC*, we surmised *acrZ* might be regulated in accordance with molybdenum levels. However, neither excess extracellular molybdenum nor lack of the ModE transcription factor or the ModABC transporter affects AcrZ–SPA accumulation (Fig. S4*A*).

We also hypothesized that *acrZ* might be coregulated with the genes encoding its interacting partners, *acrAB* and *tolC*. This hypothesis is supported by the presence of a conserved class II *mar/rob/sox* box and σ^{70} "−10" promoter region upstream of *acrZ* (Fig. 5*A*). MarA, Rob, and SoxS are highly homologous transcription factors that recognize the same consensus binding site (AYnGCACnnWnnRYYAAAY) (21) and are induced by noxious

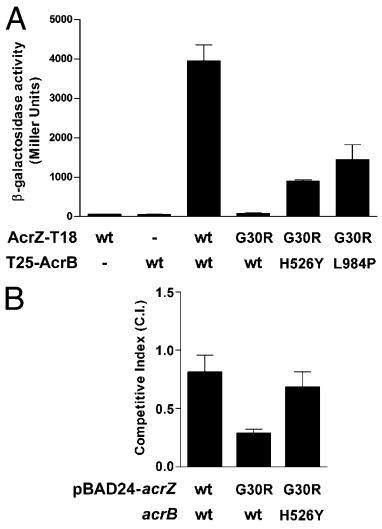

Fig. 4. Suppressor mutations in AcrB restore its interaction with $AcrZ^{G30R}$ and resistance to chloramphenicol. (*A*) $AcrB^{H526Y}$ and $AcrB^{L984P}$ but not wild-type AcrB interact with $AcrZ^{G30R}$ in a bacterial two-hybrid assay. β-Galactosidase activity was determined for cells expressing the AcrZ and AcrB proteins fused to the T18 and T25 fragments of *B. pertussis* adenylyl cyclase, respectively. High β-galactosidase activity indicates efficient reconstitution of enzyme function and affinity between the fused pair of proteins. For each strain, the enzyme activity reported is the average of three independent trials, and the error bars represent 1 SD. The levels of the wild-type and mutant derivatives of the T18 and T25 fusion proteins are comparable (Fig. S2). (*B*) Chloramphenicol resistance is restored in $AcrB^{H526Y}$ strains expressing $AcrZ^{G30R}$. Overnight cultures mixed as follows were diluted 1:2,000 into liquid LB medium: Δ*lacZ*/pBAD24 with $lacZ^+$/pBAD24-*acrZ*, Δ*lacZ*/pBAD24 with $lacZ^+$/pBAD24-$acrZ^{G30R}$, and $acrB^{H526Y}$ Δ*lacZ*/pBAD24 with $acrB^{H526Y}$ $lacZ^+$/pBAD24-$acrZ^{G30R}$. The mixed cultures were split, and one-half was treated with chloramphenicol (2 μg/mL). The reported competitive index, which represents the ratio of the tested strain to the reference strain (as measured by colony-forming units) in treated cocultures, normalized to the same ratio in mock treated cocultures (15), is the average of three independent trials, and the error bars represent 1 SD.

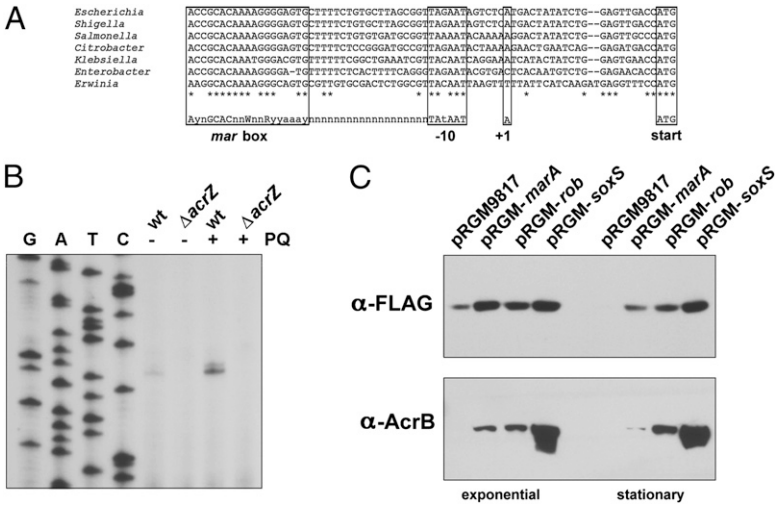

Fig. 5. *acrZ* is regulated by MarA, Rob, and SoxS. (*A*) A class II *mar*/*rob*/*sox* box is present upstream of *acrZ*. The invariant adenine at position 1 is highly conserved as is the GCAC "core" of the *mar* box (Y = C or T, R = G or A, W = A or T, and *n* = any residue; residues that match the consensus and are conserved in all sequences listed are indicated by capital letters). The 19-bp spacing of the *mar*/*rob*/*sox* box relative to the "−10" region recognized by σ^{70} is also indicative of a class II promoter structure. (*B*) Primer extension analysis of total RNA isolated from wild-type and Δ*acrZ* mutant cells treated with 250 μM paraquat for 10 min shows *acrZ* induction by paraquat. The sequencing ladder generated with the same labeled oligonucleotide used in the primer extension reactions corresponds to the strand complementary to the ORF. (*C*) Plasmids (pRGM9817) (20) constitutively expressing *marA* (pRGM-*marA*) (20), *rob* (pRGM-*rob*) (21), or *soxS* (pRGM-*soxS*) (20) were transformed into a strain containing *acrZ-SPA*. Samples were collected from each strain during the exponential and stationary phases of growth. Lysates were subjected to SDS/PAGE and immunoblot analysis to measure levels of AcrZ–SPA (α-FLAG) and AcrB (α-AcrB).

compounds such as antibiotics, detergents, and oxidizing agents. When SoxS was activated by methyl viologen (paraquat), AcrZ transcript accumulated as measured in a primer extension assay (Fig. 5*B*). This transcript initiates at a highly conserved adenine with appropriate spacing to the conserved "−10" promoter region. In addition, both AcrZ–SPA and AcrB protein levels were elevated when MarA, Rob, or SoxS were overproduced from plasmids (Fig. 5*C*).

Δ*acrZ* Mutants Are Sensitive to Many, but Not All, AcrB Substrates. In accordance with its function as an efflux pump, cells deleted for any component of the AcrAB–TolC complex are extremely sensitive to numerous antibiotics (22). Consistent with both AcrZ association with AcrB and *acrZ* regulation by MarA, Rob, and SoxS, in a recent large-scale phenotypic study designed to identify functionally related genes (23), an Δ*acrZ* mutant showed a chemical sensitivity pattern similar to deletion mutants of *acrA*, *acrB*, *rob*, and *yaiP* (which encodes a protein of unknown function). The correlation coefficient is above 0.4 for all four pairs. However, the Δ*acrZ* mutant is sensitive only to 22 of the 50 stresses under which Δ*acrB* mutants are impaired for growth in these large-scale assays (23).

To directly test Δ*acrZ* sensitivity to a subset of these compounds, we carried out competition assays between the Δ*acrZ* mutant and wild-type cells as well as between Δ*acrB* and wild-type cells (Fig. 6). As previously reported, the Δ*acrB* mutant was hypersensitive to all of the compounds tested. In contrast, Δ*acrZ* cells were hypersensitive to some compounds such as puromycin, chloramphenicol, and tetracycline, but showed wild-type sensitivity to other AcrB substrates such as erythromycin, rifampicin, and fusidic acid. This result suggests that AcrZ is required for efficient efflux of a subgroup of AcrB substrates and is dispensable for others.

We also tested the antibiotic susceptibility of the wild-type and Δ*acrZ* mutant in monoculture by minimum inhibitory concentration (MIC) assays (Table 1) and on gradient plates (Fig. S5*A*). Consistent with the results from the competition assay, Δ*acrZ* showed increased sensitivity to puromycin, chloramphenicol, and tetracycline, but not to erythromycin, rifampicin, or fusidic acid. The gradient plate assay also showed that *acrZ-SPA* fusion is phenotypically wild type. In contrast to the deletion of *acrZ*, deletions of *yajC*, which encodes another protein shown to bind AcrB (16), and of *mdtC*, *mdtF*, and *acrD*, encoding three other multidrug transporters, do not result in increased chloramphenicol or tetracycline sensitivity (Fig. S5*B*). This result, together with aforementioned findings, suggests that AcrZ uniquely binds AcrB to enhance antibiotic resistance.

Discussion

Increasing numbers of sproteins are being identified in a range of organisms, but their functions are largely unknown. Those few characterized to date act in diverse roles as toxins, intra- and intercellular signals, and effectors that modulate the activities of histidine kinases and other membrane-associated proteins (24–27). We have found that the 49-amino-acid AcrZ protein is involved in antibiotic resistance in *E. coli*. A functional AcrZ–SPA fusion associates with the highly conserved antibiotic efflux pump, AcrAB–TolC, via AcrB, the inner membrane component of the complex. Moreover, expression of *acrZ* is coregulated with *acrAB* and *tolC* by MarA, Rob, and SoxS, a set of transcription factors that regulate cellular responses to antibiotics, detergents, and redox-cycling drugs (3). Strains lacking AcrZ are sensitive to a subset of the antibiotics exported by the AcrAB–TolC pump.

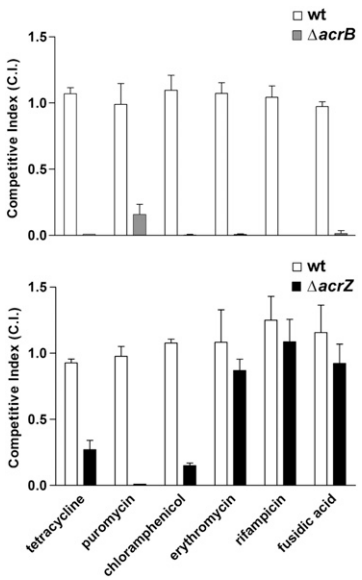

Fig. 6. Δ*acrZ* cells are hypersensitive to a subset of antibiotics to which Δ*acrB* mutants show sensitivity. Overnight cultures of otherwise wild-type Δ*lacZ* cells were mixed with either wild-type MG1655 cells or Δ*acrB* or Δ*acrZ* cells and diluted 1:2,000 in liquid LB medium. These mixed cultures were split, and one-half was treated with tetracycline (0.5 μg/mL), puromycin (45 μg/mL), chloramphenicol (2 μg/mL), erythromycin (60 μg/mL), rifampicin (5 μg/mL), or fusidic acid (60 μg/mL). The reported competitive index is as in Fig. 4. The predicted partition coefficients XlogP3 (PubChem) for the antibiotics are −2, 0, 1.1, 2.7, 4.0, and 5.5, respectively.

Table 1. MIC (μg/mL) of wild type, Δ*acrZ*, and Δ*acrB* single mutants and Δ*acrZ* Δ*acrB* double mutant

	Tetracycline	Puromycin	Chloramphenicol	Erythromycin	Rifampicin	Fusidic acid
Wild type	2	400	8	50	24	5,000
Δ*acrZ*	1.5	200	4	50	24	5,000
Δ*acrB*	1	12.5	1	3.13	16	16
Δ*acrB* Δ*acrZ*	1	12.5	1	3.13	16	16

The N-terminal end of AcrZ exhibits some homology with the TM2 of AcrB (Fig. S3*A*), suggesting that AcrZ may have co-opted an interaction surface from its target AcrB. Consistent with this hypothesis, one of the two mutations that could suppress the AcrZ dominant-negative mutant is in the L984 residue, which is in close proximity to TM2 of AcrB (Fig. S3*B*). We speculate that AcrZ could be acting by imitating one TM helix of its partner, possibly binding to AcrB by substituting for TM2 or inserting between TM2 and TM11.

The fact that Δ*acrZ* cells are sensitive to some but not all of the antimicrobial agents that affect Δ*acrB* cells suggests that AcrZ affects the specificity of drug export. Recent studies on the crystal structure of substrate bound AcrB (28–30) and biochemical mapping of the substrate path (31, 32) have shown that there are multiple drug-binding sites in the large periplasmic domain of AcrB. We propose that AcrZ binding to AcrB could trigger conformational changes in the periplasmic domain, thus directly affecting the recognition and capture of certain substrates, such as substrates with lower hydrophobicity (Fig. 6). Alternatively or additionally AcrZ may interact with other single-component transport proteins proposed to collaborate with AcrAB–TolC (33) to promote the delivery of drugs to AcrB, which subsequently clears the drug from the periplasmic space.

As mentioned above, *acrZ* shares strong synteny with two flanking operons involved in molybdenum uptake and the regulation of molybdenum cofactor synthesis. We note that the structures of many polycyclic substrates for AcrB, such as tetracycline and acriflavine, are reminiscent of the molybdenum cofactor. In addition, molybdenum cofactor-containing enzymes, such as xanthine dehydrogenase and aldehyde oxidoreductase, detoxify compounds that may potentially be exported by AcrB. We did not observe any defects associated with molybdenum deficiency such as loss of chlorate susceptibility (Fig. S4*B*) or increased sensitivity to aromatic aldehydes in an *acrZ* mutant strain (Fig. S4*C*). However, it is still possible that the synteny between *acrZ* and the molybdenum operons is driven by a possible role for AcrZ in enabling AcrB to remove the various forms of molybdenum cofactor or substrates of molybdo-enzymes.

Interestingly, AcrB previously was found to associate with YajC, another relatively small TM protein (110 amino acids) in structural studies of AcrB (16). YajC is encoded within an operon that also codes for the RND family member SecDF and is part of the SecDF–YajC complex that facilitates protein secretion via SecYEG. The most highly conserved residues of YajC reside in its TM α-helix and were found to interact with a highly conserved binding pocket along the TM surface of AcrB (16). Δ*yajC* cells were reported to be mildly sensitive to certain β-lactam antibiotics. The basis for YajC-mediated sensitivity to β-lactam antibiotics was not apparent from the structural data, but it will be of interest to examine the similarities and differences between the AcrZ and YajC interactions with AcrB.

RND proteins are found throughout all domains of life and could be a rich set of targets for small membrane proteins in both bacterial and eukaryotic systems. Like the example of AcrZ discussed here, small proteins associated with these transporters most likely have been overlooked due to experimental challenges in their detection. Future investigations of AcrZ and other as-yet-undiscovered sproteins that interact with RND family members will help illuminate how sproteins might alter the ability of these important pumps to recognize and transport substrates, which ultimately may be invaluable for developing therapies to either limit or promote RND activity.

Materials and Methods

Strain Construction. All strains are derivatives of the laboratory stock of *E. coli* K-12 MG1655 unless otherwise noted and are listed in Dataset S1. The plasmids and oligonucleotides used in this study are listed in Datasets S2 and S3, respectively. Chromosomal mutants were generated by using λ-Red–mediated recombineering (34, 35). Details about strain construction and genetic screens are provided in *SI Materials and Methods*.

Bacterial Growth. Cells were propagated in standard fashion in liquid or on solid [1.5% (wt/vol) Bacto-agar] Luria–Bertani media (10 g of tryptone, 5 g of yeast extract, 10 g of NaCl per liter). Glucose and arabinose were used at concentrations of 0.2% (wt/vol). Antibiotics were used at the following concentrations for selection of marker genes: kanamycin, 30 μg/mL; chloramphenicol, 25 μg/mL; ampicillin, 100 μg/mL; and tetracycline, 12.5 μg/mL.

Competition Assays and MIC Assays. Competition assays were performed as in ref. 15, and MIC assays were performed by serial agar dilutions as in ref. 22 with minor modifications. These antibiotic sensitivity assays are described in detail in *SI Materials and Methods*.

AcrZ–SPA and AcrB–His_6 Purification and Detection. The SPA and His_6-tagged proteins were purified on the basis of their tags and the tagged proteins as well as untagged AcrB were detected by immunoblot analysis as described in detail in *SI Materials and Methods*.

Bacterial Two-Hybrid Assays. Pairs of proteins to be tested were fused to the two catalytic domains T18 and T25 of adenylate cyclase based on their confirmed topologies. The resulting plasmids were cotransformed into a Δ*cya* strain, and transformants were grown in LB medium supplemented with ampicillin, kanamycin, and 0.5 mM isopropyl-β-D-thiogalactopyranoside for 16 h at 30 °C. The overnight cultures (1 mL) were harvested and assayed for β-galactosidase activity as described (36).

Primer Extension Assays. Cultures of wild-type MG1655 and Δ*acrZ* cells grown to mid-exponential phase (OD_{600} ~0.4–0.6) were split, and half of the culture was exposed to 250 μM paraquat for 10 min. Total RNA was extracted by hot acid phenol as described previously (37). Primer extension analysis was carried out using 5′-end, ^{32}P-labeled primer (1 pmol) and total RNA (5 μg) as described previously (38).

ACKNOWLEDGMENTS. We thank P. Backlund and A. Yergey for conducting the mass spectrometric analysis; A. Battesti, N. Majdalani, H. Nikaido, L. Rosner, and A. Sharma for sharing antisera, strains, and plasmids; and M. Goulian, M. Machner, K. Ramamurthi, and L. Rosner for comments on the manuscript. Work in the laboratory of G.S. is supported by the Intramural Program of the Eunice Kennedy Shriver National Institute of Child Health and Human Development. E.C.H. was additionally supported by the Pharmacology Research Associate Program of the National Institute of General Medical Sciences and B.J.P. was supported by a fellowship from the National Research Council.

1. Otto M (2010) Looking toward basic science for potential drug discovery targets against community-associated MRSA. *Med Res Rev* 30:1–22.
2. Nikaido H, Pagès JM (2012) Broad-specificity efflux pumps and their role in multidrug resistance of Gram-negative bacteria. *FEMS Microbiol Rev* 36:340–363.
3. Grkovic S, Brown MH, Skurray RA (2002) Regulation of bacterial drug export systems. *Microbiol Mol Biol Rev* 66:671–701.
4. Randall LP, Woodward MJ (2002) The multiple antibiotic resistance (mar) locus and its significance. *Res Vet Sci* 72:87–93.

5. Blair JM, Piddock LJ (2009) Structure, function and inhibition of RND efflux pumps in Gram-negative bacteria: An update. *Curr Opin Microbiol* 12:512–519.
6. Murakami S, Nakashima R, Yamashita E, Matsumoto T, Yamaguchi A (2006) Crystal structures of a multidrug transporter reveal a functionally rotating mechanism. *Nature* 443:173–179.
7. Seeger MA, et al. (2006) Structural asymmetry of AcrB trimer suggests a peristaltic pump mechanism. *Science* 313:1295–1298.
8. Lomovskaya O, Zgurskaya HI, Totrov M, Watkins WJ (2007) Waltzing transporters and 'the dance macabre' between humans and bacteria. *Nat Rev Drug Discov* 6:56–65.
9. Piddock LJ (2006) Multidrug-resistance efflux pumps—not just for resistance. *Nat Rev Microbiol* 4:629–636.
10. Hobbs EC, Fontaine F, Yin X, Storz G (2011) An expanding universe of small proteins. *Curr Opin Microbiol* 14:167–173.
11. Hemm MR, Paul BJ, Schneider TD, Storz G, Rudd KE (2008) Small membrane proteins found by comparative genomics and ribosome binding site models. *Mol Microbiol* 70: 1487–1501.
12. Hemm MR, et al. (2010) Small stress response proteins in *Escherichia coli*: Proteins missed by classical proteomic studies. *J Bacteriol* 192:46–58.
13. Fontaine F, Fuchs RT, Storz G (2011) Membrane localization of small proteins in *Escherichia coli*. *J Biol Chem* 286:32464–32474.
14. Zeghouf M, et al. (2004) Sequential Peptide Affinity (SPA) system for the identification of mammalian and bacterial protein complexes. *J Proteome Res* 3:463–468.
15. Hobbs EC, Astarita JL, Storz G (2010) Small RNAs and small proteins involved in resistance to cell envelope stress and acid shock in *Escherichia coli*: Analysis of a barcoded mutant collection. *J Bacteriol* 192:59–67.
16. Törnroth-Horsefield S, et al. (2007) Crystal structure of AcrB in complex with a single transmembrane subunit reveals another twist. *Structure* 15:1663–1673.
17. Guzman LM, Belin D, Carson MJ, Beckwith J (1995) Tight regulation, modulation, and high-level expression by vectors containing the arabinose P_{BAD} promoter. *J Bacteriol* 177:4121–4130.
18. Karimova G, Pidoux J, Ullmann A, Ladant D (1998) A bacterial two-hybrid system based on a reconstituted signal transduction pathway. *Proc Natl Acad Sci USA* 95: 5752–5756.
19. Mendel RR, Bittner F (2006) Cell biology of molybdenum. *Biochim Biophys Acta* 1763: 621–635.
20. Martin RG, Gillette WK, Rosner JL (2000) Promoter discrimination by the related transcriptional activators MarA and SoxS: Differential regulation by differential binding. *Mol Microbiol* 35:623–634.
21. Martin RG, Gillette WK, Martin NI, Rosner JL (2002) Complex formation between activator and RNA polymerase as the basis for transcriptional activation by MarA and SoxS in *Escherichia coli*. *Mol Microbiol* 43:355–370.
22. Sulavik MC, et al. (2001) Antibiotic susceptibility profiles of *Escherichia coli* strains lacking multidrug efflux pump genes. *Antimicrob Agents Chemother* 45:1126–1136.
23. Nichols RJ, et al. (2011) Phenotypic landscape of a bacterial cell. *Cell* 144:143–156.
24. Alix E, Blanc-Potard AB (2009) Hydrophobic peptides: Novel regulators within bacterial membrane. *Mol Microbiol* 72:5–11.
25. Eguchi Y, et al. (2007) B1500, a small membrane protein, connects the two-component systems EvgS/EvgA and PhoQ/PhoP in *Escherichia coli*. *Proc Natl Acad Sci USA* 104:18712–18717.
26. Lippa AM, Goulian M (2009) Feedback inhibition in the PhoQ/PhoP signaling system by a membrane peptide. *PLoS Genet* 5:e1000788.
27. Modell JW, Hopkins AC, Laub MT (2011) A DNA damage checkpoint in *Caulobacter crescentus* inhibits cell division through a direct interaction with FtsW. *Genes Dev* 25: 1328–1343.
28. Nakashima R, Sakurai K, Yamasaki S, Nishino K, Yamaguchi A (2011) Structures of the multidrug exporter AcrB reveal a proximal multisite drug-binding pocket. *Nature* 480: 565–569.
29. Takatsuka Y, Chen C, Nikaido H (2010) Mechanism of recognition of compounds of diverse structures by the multidrug efflux pump AcrB of *Escherichia coli*. *Proc Natl Acad Sci USA* 107:6559–6565.
30. Eicher T, et al. (2012) Transport of drugs by the multidrug transporter AcrB involves an access and a deep binding pocket that are separated by a switch-loop. *Proc Natl Acad Sci USA* 109:5687–5692.
31. Husain F, Bikhchandani M, Nikaido H (2011) Vestibules are part of the substrate path in the multidrug efflux transporter AcrB of *Escherichia coli*. *J Bacteriol* 193:5847–5849.
32. Husain F, Nikaido H (2010) Substrate path in the AcrB multidrug efflux pump of *Escherichia coli*. *Mol Microbiol* 78:320–330.
33. Tal N, Schuldiner S (2009) A coordinated network of transporters with overlapping specificities provides a robust survival strategy. *Proc Natl Acad Sci USA* 106: 9051–9056.
34. Datsenko KA, Wanner BL (2000) One-step inactivation of chromosomal genes in Escherichia coli K-12 using PCR products. *Proc Natl Acad Sci USA* 97:6640–6645.
35. Yu D, et al. (2000) An efficient recombination system for chromosome engineering in *Escherichia coli*. *Proc Natl Acad Sci USA* 97:5978–5983.
36. Miller JH (1992) *A Short Course in Bacterial Genetics: A Laboratory Manual and Handbook for Escherichia coli and Related Bacteria* (Cold Spring Harbor Laboratory Press, Plainview, NY).
37. Massé E, Escorcia FE, Gottesman S (2003) Coupled degradation of a small regulatory RNA and its mRNA targets in *Escherichia coli*. *Genes Dev* 17:2374–2383.
38. Opdyke JA, Kang JG, Storz G (2004) GadY, a small-RNA regulator of acid response genes in *Escherichia coli*. *J Bacteriol* 186:6698–6705.